Rapid Large-Area Multiphoton Microscopy for Characterization of Graphene

Antti Säynätjoki,[†,*] Lasse Karvonen,[†] Juha Riikonen,[†] Wonjae Kim,[†] Soroush Mehravar,[‡] Robert A. Norwood,[‡] Nasser Peyghambarian,[‡] Harri Lipsanen,[†] and Khanh Kieu[‡]

[†]Department of Micro and Nanosciences, Aalto University, Tietotie 3, FI-02150 Espoo, Finland and [‡]College of Optical Sciences, University of Arizona, 1630 E. University Boulevard, Tucson, Arizona 85721, United States

ABSTRACT Single- and few-layer graphene was studied with simultaneous third-harmonic and multiphoton-absorption-excited fluorescence microscopy using a compact 1.55 μm mode-locked fiber laser source. Strong third-harmonic generation (THG) and multiphoton-absorption-excited fluorescence (MAEF) signals were observed with high contrast over the signal from the substrate. High contrast was also achieved between single- and bilayer graphene. The measurement is straightforward and very fast compared to typical Raman mapping, which is the conventional method for characterization of graphene. Multiphoton microscopy is also proved to be an extremely efficient method for detecting certain structural features in few-layer graphene. The accuracy and speed of multiphoton microscopy make it a very promising characterization technique for fundamental research as well as large-scale fabrication of graphene. To our knowledge, this is the first time simultaneous THG and MAEF microscopy has been utilized in the characterization of graphene. This is also the first THG microscopy study on graphene using the excitation wavelength of 1.55 μm, which is significant in telecommunications and signal processing.

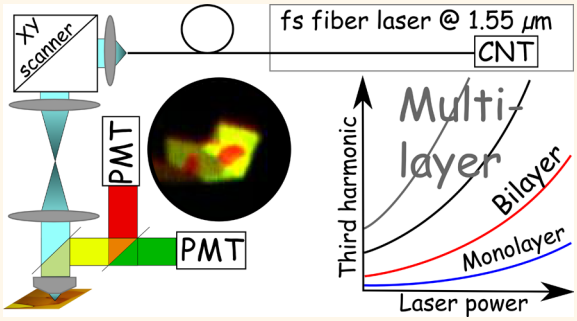

KEYWORDS: graphene · multiphoton microscopy · third-harmonic generation · multiphoton excitation fluorescence

Graphene exhibits unique optical and electrical properties, and since its discovery in the early 2000s, graphene has been studied extensively.[1,2] Its peculiar properties make it a unique material for a variety of applications such as field-effect transistors,[3] nonlinear rectifiers,[4] supercapacitors,[5] filter membranes,[6] biomedical sensors,[7] and touch screens.[8] The massless quasiparticle states in graphene open up new ways to study quantum relativistic phenomena.[9,10] In these studies, nonlinear optical response of graphene is one of the key issues. Graphene has also been utilized in various optical applications, such as optical modulation[11] and photodetection,[12] as a saturable absorber for laser mode-locking,[13] and as a third-order nonlinear optical material to generate optical bistability, regenerative oscillations, and four-wave mixing.[14] For successful device fabrication it is crucial to characterize the graphene quality to ensure best device performance and yield. Standard characterization methods for graphene include Raman microscopy, optical microscopy, atomic force microscopy (AFM), scanning tunneling microscopy (STM), scanning electron microscopy (SEM), and transmission electron microscopy (TEM). The contrast produced by graphene in optical microscopy is weak (the absorption of single-layer graphene is only 2.3%),[15] and therefore special substrates are commonly used to enhance optical contrast. Raman microscopy is probably the most important and widely used tool for graphene characterization since it can be used to assess the quality of graphene, *e.g.*, number of layers, strain, doping, interlayer interaction, and defects.[16−19] However, spectral Raman microscopy is currently quite time-consuming, which may prohibit its use in rapid characterization of large-area graphene samples needed for many applications. Furthermore, the focused laser beam used in Raman mapping may even damage the sample especially during detailed spatial mapping.

* Address correspondence to antti.saynatjoki@aalto.fi.

Received for review March 21, 2013 and accepted September 11, 2013.

Published online September 12, 2013
10.1021/nn4042909

Multiphoton imaging (MPI) is a powerful technique that allows mapping of samples that have any kind of nonlinear optical response such as second-harmonic generation (SHG), third-harmonic generation (THG), or fluorescence induced by multiphoton (MP) absorption.[20−23] While multiphoton-absorption-excited fluorescence,[24,25] second-harmonic generation,[26] and, very recently, third-harmonic generation[27,28] in graphene have been studied, the full potential of this versatile technique has not yet been exploited.

Optical nonlinearities are the basis of all-optical devices that are important in telecommunications networks. The previous work on third-harmonic generation in graphene has been carried out at the wavelengths of 800 nm[27] and 1.72 μm.[28] To directly assess the potential of using graphene in telecommunications devices, it is crucial to study its nonlinear response at telecommunications wavelengths around 1.55 μm. The long excitation wavelength also yields a third-harmonic signal in the visible wavelength range, where high-sensitivity photomultiplier tubes (PMT) exist.

In this work, we have successfully employed multiphoton microscopy with a compact 1.55 μm femtosecond fiber laser to study the nonlinear optical properties of single- and few-layer graphene. We also compare this method with Raman mapping and standard optical imaging. In contrast to standard optical microscopy, multiphoton microscopy relies on the nonlinear optical properties of the material, yielding high-contrast signals without special sample preparation. We further established that the third-harmonic signal is very sensitive to certain structural features in graphene that are barely detectable by Raman microscopy. The technique is very fast compared to Raman mapping and is far better suited for characterization of samples with large surface areas. Therefore, multiphoton microscopy constitutes an efficient new tool for the characterization of graphene, particularly for large-scale CVD-deposited graphene films and device characterization. To our knowledge, this is the first THG and multiphoton-absorption-excited fluorescence (MAEF) microscopy study of graphene using laser excitation wavelengths in the telecommunication range near 1.55 μm.

RESULTS AND DISCUSSION

Multiphoton Microscope. Second- and third-harmonic signals and multiphoton-absorption fluorescence from graphene samples were measured using the multiphoton microscope shown schematically in Figure 1. A femtosecond laser beam with a wavelength of 1.55 μm is scanned in the *xy*-plane with a dual-axis mirror system and focused on the sample using a microscope objective. The backscattered light is split into two branches using a long-pass dichroic mirror (cutoff at 562 nm) and then detected using PMTs. Bandpass

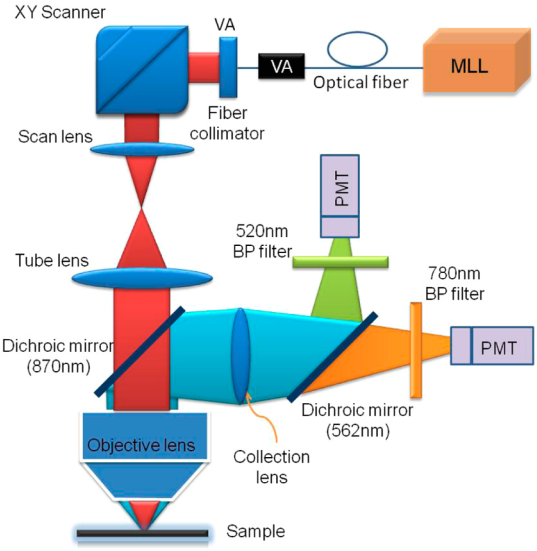

Figure 1. Schematic diagram of the multiphoton microscope. MLL: mode-locked fiber laser with a carbon nanotube saturable absorber. VA: variable attenuator. BP filter: bandpass filter.

filters were used to separate different spectral windows of the backscattered signal. Specifically, a 520 ± 10 nm filter enables measurements of third-harmonic generated signal, a 780 ± 10 nm bandpass filter is used to measure second-harmonic emission from the sample, and fluorescence due to two- or three-photon excitation can be measured using just the dichroic long-pass filter without the 780 nm bandpass filter.

Large-Area Characterization. Figure 2 shows large-area multiphoton micrographs of an exfoliated graphene area. The images are taken using a 10×, 0.45 NA objective. This moderate magnification allows a relatively large area of approximately 450 × 450 μm^2 to be imaged. The image on the left in Figure 2 is the MAEF image, obtained with the PMT that receives light of wavelength longer than 562 nm that passed through the dichroic mirror. The image in the center is based on the third-harmonic signal obtained using the 520 nm bandpass filter located in the branch where the wavelengths below 562 nm were directed. All the graphite pieces on the sample are clearly visible in both images. More importantly, the few-layer graphene flake that is marked with the white circle in the fluorescence image is also clearly visible. It is nearly as bright as the significantly thicker bulk graphite that is typical of the exfoliation method. We also measured fluorescence using an 801 nm long-pass filter to compare the fluorescence intensity at different spectral regimes. The fluorescence signal between 562 and 801 nm was about 7 times stronger than that between 801 and 920 nm. Taking into account the wavelength-dependent sensitivity of the PMT we used, this ratio is in good agreement with the spectra discussed in ref 24.

The resolution of the microscope is determined mainly by the numerical aperture (NA) of the objective.

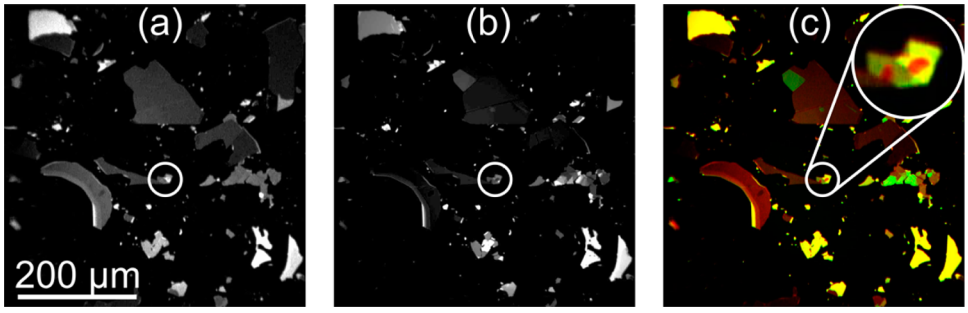

Figure 2. Typical multiphoton micrographs of a sample containing exfoliated graphene on SiO_2/Si substrate. (a) fluorescence, (b) third-harmonic signal, and (c) merged RGB image using fluorescence (red) and THG (green) signals. One particularly interesting few-layer graphene flake considered below is marked with white circles and shown magnified in the merged RGB image.

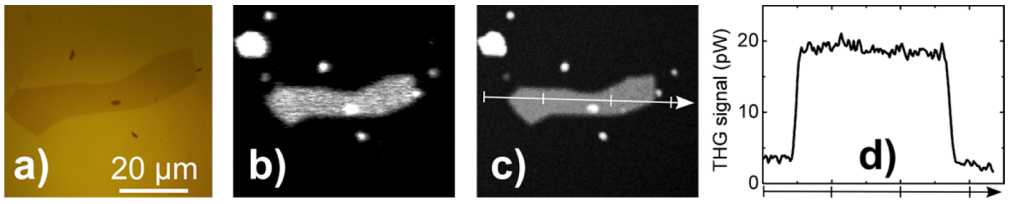

Figure 3. Microscope images of single-layer exfoliated graphene. (a) optical, (b) MAEF, (c) THG, and (d) the THG intensity profile along the white arrow in part c.

With the 10× and 0.45 NA objective we used in our experiment, the resolution is 1.85 μm in the *xy*-plane and ~10 μm on the vertical *z*-axis, as measured using the nonlinear knife-edge technique.

Simultaneous multichannel detection makes multiphoton microscopy a powerful tool for material characterization. Figure 2c shows an image, where the red channel is from the MAEF signal in Figure 2a, and the green channel in the red-green-blue (RGB) image originates from the THG signal shown in Figure 2b. In this kind of composite image, MAEF and THG intensive areas are red and green, respectively. The areas with high intensity for both the THG and fluorescence appear yellow in the composite image. Green, red, and yellow areas are all seen where the few-layer graphene flake is located; these features will be discussed in more detail below.

Single-Layer Graphene. Figure 3 shows the standard optical, MAEF, and THG images of a single-layer graphene flake. The fluorescence and THG signals generated in the single-layer graphene, shown in Figure 3b and c, respectively, are both clearly distinguishable from the background. The THG signal, plotted in Figure 3d, is nearly constant over the whole single-layer graphene flake with a length of more than 50 μm. As seen in Figure 3, multiphoton microscopy provides significantly better contrast compared to standard optical microscopy, even though we used a special substrate (300-nm-thick SiO_2/Si) to maximize the optical contrast.[29] The THG signal on graphene is about 20 pW, while it is about 3 pW on the substrate. In this case, the substrate signal arises mainly from the silicon beneath the thin SiO_2 layer. As silicon is not transparent for the visible THG light, only light generated within the extinction length can be seen. Using the relation[30]

$$\frac{|\chi^{(3)}_{gr}|}{|\chi^{(3)}_{Si}|} = \frac{d_{Si}}{d_{gr}}\sqrt{\frac{I_{gr}}{I_{Si}}}$$

where d_{gr} and d_{Si} are the estimated graphene thickness (0.335 nm) and extinction length of 520 nm light in silicon (~1 μm; ref 31), respectively, and I_{gr} and I_{Si} are the THG signals on and off the graphene flake, respectively, we estimate that $\chi^{(3)}$ for single-layer graphene is about 8000 times $\chi^{(3)}$ of silicon. With $\chi^{(3)} = 4 \times 10^{-11}$ esu for silicon,[32] this yields $\chi^{(3)} \approx 3 \times 10^{-7}$ esu for single-layer graphene. This is in good agreement with an earlier estimate based on four-wave mixing experiments at wavelengths near 800 nm.[30]

Few-Layer Graphene. Figure 4a shows an optical micrograph of the few-layer exfoliated graphene flake highlighted in Figure 2. Areas with different levels of optical absorption, corresponding to a different number of graphene layers, can be distinguished. According to Raman spectroscopy, the area marked with number "1" in Figure 4a is bilayer graphene, while the darker areas have a larger number of graphene layers. Figure 4b and c show the multiphoton micrographs of the same area. A few dark spots are the main difference between the optical and THG images and will be discussed in more detail below. The fluorescence image in the lower part of Figure 4c shows that the strongest fluorescence can be seen in regions where the absorption is higher (darker areas in Figure 4a); therefore, MAEF is stronger with an increasing number of graphene layers. The second-harmonic signal is generally weak, with the

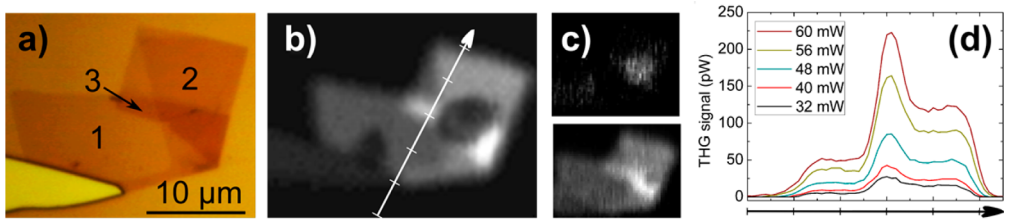

Figure 4. Optical and multiphoton microscope images of few-layer exfoliated graphene. (a) Optical, (b) THG, (c) top, SHG; bottom, MAEF, and (d) the THG signal along the arrow in part b with different excitation powers.

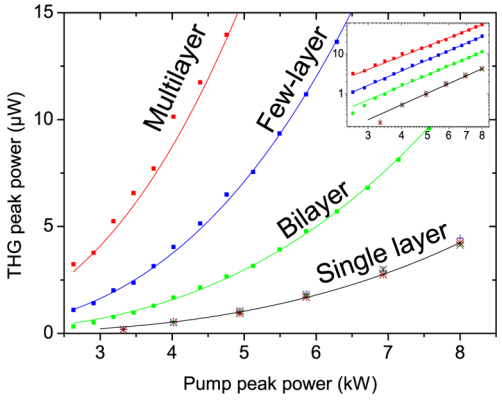

Figure 5. Dependence of the THG peak signal on the laser peak power and number of graphene layers. Dots are measurement values; the curves are exponential fits to the power dependence. Multi-, few-, and bilayer plots correspond to areas 1, 2, and 3 in Figure 4a, respectively. For single layers, measurements from four different flakes are shown as different symbols. In the logarithmic plot in the inset, three points corresponding to the lowest THG power deviate from the general trend because the power level is below the linear regime of our detection system.

exception of a few locations, which coincide with the dark spots in the third-harmonic image. Figure 4d presents the THG signal profile along a line crossing areas (in Figure 4b) with different numbers of graphene layers. The signal is constant over areas with the same number of graphene layers, generally increasing with the number of graphene layers.

Power Dependence. The dependence of the THG signal on the excitation power was studied by imaging several graphene flakes with different numbers of graphene layers. The signals were generated using the few-layer areas labeled 1, 2, and 3 in Figure 4a and from several single-layer graphene flakes, one of which is shown in Figure 3. All single-layer graphene areas showed very consistent THG signals, as can be seen in Figure 5. The third-harmonic signal generated in different single-layer graphene flakes exhibits a strikingly similar power dependence, and it is clearly distinguishable from the trend for bilayer and multilayer graphene regions. The fit lines in Figure 5 follow the power law equation $P_{THG} = aP_p^b$, where P_{THG} and P_p are the THG and pump powers, respectively, and the coefficient a and exponent b are set for the best fit to the data. Consistent with the theory, the third-harmonic signal from the single-layer graphene has a cubic dependence on the excitation peak power, *i.e.*, $b \approx 3$. For a larger number of layers, the power dependence of THG is subcubic: for bilayer and few-layer areas, $b \approx 2.85$, and for the multilayer area, $b \approx 2.55$. The decreasing exponent for the multilayer graphene can be best seen in the logarithmic plot in the inset in Figure 5.

The fluorescence signal has a quadratic dependence on the excitation power for single- and bilayer graphene, as also observed in a previous study for high fluence.[24] In this case, the quadratic dependence occurs as a function of average power, *i.e.*, pulse energy, not peak power, as was the case for THG. The reason for this difference is that fluorescence occurs as a result of multiple photons exciting electrons in graphene, as discussed in ref 24. Therefore, excited electrons for fluorescence may accumulate during the pulse, whereas THG is an instantaneous process arising directly from the optical field. For areas that are thicker than bilayer, both fluorescence and THG depend on the excitation power to a smaller exponent than predicted. The origin of this phenomenon could be related to the accumulation of nonlinear effects (*e.g.*, nonlinear refractive index) in the multilayer graphene.

THG-Sensitive Features in Graphene. Raman mapping was carried out to further characterize the locations with dark spots in the third-harmonic image. In the Raman maps in Figure 6, we can see some variation in areas whose location and shape have a perfect match to the dark spots in the THG image (Figure 4b). Specifically, the intensity of the G and 2D (also known as G′[18]) band signals have a slight *increase* compared to the surrounding areas, as shown in Figure 6a and b, respectively. Most importantly, the disorder-induced D peak cannot be observed in these areas in Figure 6c (only at the edges due to symmetry-breaking effect). This suggests that the features in THG and Raman images do not arise from defects in the graphene layers. In our experiments we did not observe such features in single-layer graphene. Therefore, it is conceivable that the change may be related to a variation of the bonding between graphene sheets in the bi- and multilayer graphene areas. The appearance of the SHG signal also suggests the presence of non-centrosymmetry at these very same locations. Bonding between layers has been predicted and observed to change under intense laser radiation.[33] Raman spectroscopy as

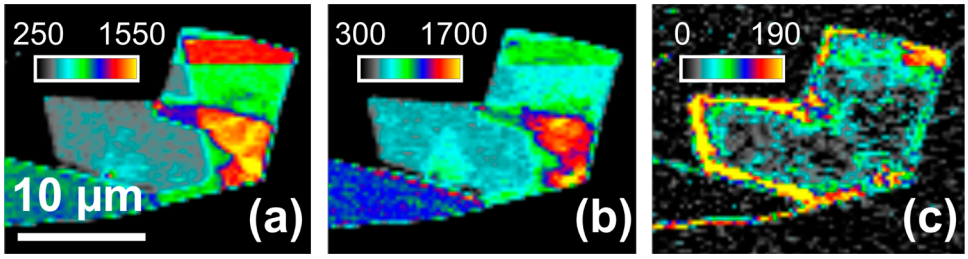

Figure 6. Raman maps of the few-layer graphene area under study. (a) G line, (b) 2D (G′) line, and (c) D line.

well as multiphoton microscopy uses high-intensity lasers that can potentially alter graphene. Even though the laser fluence used in our multiphoton microscope is below the threshold values found by Jeschke *et al.*,[33] the effects of persistent laser fluence on graphene, as experienced during extensive multiphoton microscopy as well as Raman spectroscopy, may be worth further investigation. While the exact origin of the features remains unclear, it is evident that these differences can be easily and rapidly observed in multiphoton microscopy, whereas they are very subtle in Raman spectroscopy and only visible after tedious data processing. Systematic study considering the origin and formation of these features is under way.

Rapid Characterization. Our study shows that multiphoton microscopy is a promising technique for rapid characterization of graphene. While graphene fabrication has seen tremendous development, even roll-to-roll production,[8] characterization of graphene is still a time-consuming task that may even become a bottleneck in real-time monitoring of high-volume manufacturing processes. Therefore, simple, fast, and efficient graphene characterization methods are needed. Compared to Raman spectroscopy, which is currently the most commonly used method for graphene characterization, multiphoton microscopy is very fast. In our work, an area of 450 × 450 μm (1024 lines of 1024 points each) can be imaged with the multiphoton microscope in about 5 s or less, whereas Raman mapping of an area of 25 × 25 μm (120 lines, 120 points each) takes about 12 min. In addition, a video rate multiphoton microscope is feasible by using faster scanning mirrors and/or by increasing laser peak power. Single-layer, bilayer, and multilayer graphene may be distinguished in the images by using the signal level. This is very useful, for example, when analyzing large-scale single-layer CVD graphene, which typically contains parasitic flakes (adlayer domains).[34] Therefore, multiphoton microscopy demonstrates great potential to be a very efficient characterization tool for large-scale fabricated graphene. Once the process is optimized for maximal optical throughput, the laser exposure will also be minimized.

CONCLUSIONS

We have demonstrated that multiphoton microscopy is a very efficient method for characterizing single- and few-layer graphene. Compared to Raman mapping, this method is very rapid. Unlike in standard optical microscopy, no special sample preparation is needed. High contrast between single-layer, bilayer, and multilayer graphene is readily achieved. We believe that this method has a significant potential for fundamental research on graphene as well as for large-scale graphene characterization, which is crucial for ensuring high yield and high throughput in the fabrication of graphene devices.

METHODS

Graphene flakes were deposited on oxidized silicon substrates using the exfoliation method.[35] The thickness of the thermal SiO_2 was set to 300 nm to achieve maximal contrast in standard optical microscopy. Single- and few-layer graphene areas were first identified using optical microscopy and then confirmed by Raman spectroscopy.

The multiphoton microscope setup for the characterization of second- and third-harmonic signals and multiphoton-absorption fluorescence is shown schematically in Figure 1. The excitation laser source in the system is an amplified erbium-doped mode-locked fiber laser operating at the central wavelength of 1.55 μm.[36] The light is delivered to the microscope using an optical fiber. The seed laser oscillator is mode-locked using a carbon nanotube saturable absorber similar to the one reported in ref 37. The maximum average power of the laser is 60 mW at the sample surface, and the repetition rate is ~50 MHz. The pulse duration on the sample depends on the average power due to soliton compression effects in the delivery fiber. The pulse duration is ~150 fs at an average power of 60 mW, and it increases gradually to ~280 fs at an average power of 10 mW. The pulse peak power has been calculated accordingly. The peak power and pulse energy at an average power of 60 mW are 8 kW and 1.2 nJ, respectively. To produce an image, the laser beam is scanned in the *xy*-plane with a dual-axis galvo mirror system and focused on the sample using a microscope objective. With the 10× objective used in this work, the laser spot size was 1.85 μm, yielding a peak intensity of 300 GW/cm^2 on the sample. The backscattered light is split into two branches using a long-pass dichroic mirror (cutoff at 562 nm) and then detected using PMTs. The multialkaline-based PMTs (Hamamatsu H10721-20) detect light only up to a wavelength of 0.92 μm, thus preventing the excitation light from being detected. The paths to the two PMTs can be equipped with different bandpass filters to analyze different spectral windows of the backscattered signal. Specifically, we used a 520 ± 10 nm bandpass filter in order to detect third-harmonic emission from the sample. In the other channel, a 780 ± 10 nm bandpass filter allows detection of the second-harmonic signal generated in the sample, while with just the dichroic long-pass filter without the 780 nm bandpass filter,

detection of fluorescence signal due to two- or three-photon excitation is enabled.

Raman spectra and maps were collected using confocal micro-Raman spectroscopy with a 532 nm Nd:YAG laser. The maps were measured using 120 points × 120 lines for the area of 25 μm × 25 μm.

Conflict of Interest: The authors declare no competing financial interest.

Acknowledgment. The work is financed by the Academy of Finland, TEKES—the Finnish Funding Agency for Technology and Innovation, the Graduate School of Modern Optics and Photonics, the Finnish Foundation for Technology Promotion, and the Walter Ahlström Foundation. We also acknowledge the provision of technical facilities of the Micronova, Nanofabrication Centre of Aalto University. University of Arizona contributors would like to acknowledge the support of the AFOSR COMAS MURI (FA9550-10-1-0558), the CIAN NSF ERC under grant EEC-0812072, and TRIF Photonics funding from the state of Arizona.

REFERENCES AND NOTES

1. Bonaccorso, F.; Lombardo, A.; Hasan, T.; Sun, Z.; Colombo, L.; Ferrari, A. C. Production and Processing of Graphene and 2d Crystals. *Mater. Today* **2012**, *15*, 564–589.
2. Novoselov, K. S.; Falko, V. I.; Colombo, L.; Gellert, P. R.; Schwab, M. G.; Kim, K. A Roadmap for Graphene. *Nature* **2012**, *490*, 192–200.
3. Wu, Y.; Lin, Y.-M.; Bol, A. A.; Jenkins, K. A.; Xia, F.; Farmer, D. B.; Shu, Y.; Avouris, P. High-Frequency, Scaled Graphene Transistors on Diamond-Like Carbon. *Nature* **2011**, *472*, 74–78.
4. Kim, W.; Pasanen, P.; Riikonen, J.; Lipsanen, H. Nonlinear Behavior of Three-Terminal Graphene Junctions at Room Temperature. *Nanotechnology* **2012**, *23*, 115201.
5. Liu, C.; Yu, Z.; Neff, D.; Zhamu, A.; Jang, B. Z. Graphene-Based Supercapacitor with an Ultrahigh Energy Density. *Nano Lett.* **2010**, *10*, 4863–4868.
6. Nair, R. R.; Wu, H. A.; Jayaram, P. N.; Grigorieva, I. V.; Geim, A. K. Unimpeded Permeation of Water through Helium-Leak—Tight Graphene-Based Membranes. *Science* **2012**, *335*, 442–444.
7. He, S.; Song, B.; Li, D.; Zhu, C.; Qi, W.; Wen, Y.; Wang, L.; Song, S.; Fang, H.; Fan, C. A Graphene Nanoprobe for Rapid, Sensitive, and Multicolor Fluorescent DNA Analysis. *Adv. Funct. Mater.* **2010**, *20*, 453–459.
8. Bae, S.; Kim, H.; Lee, Y.; Xu, X.; Park, J.-S.; Zheng, Y.; Balakrishnan, J.; Lei, T.; Kim, H.; Song, Y.; Kim, Y.; *et al.* Roll-to-Roll Production of 30-Inch Graphene Films for Transparent Electrodes. *Nat. Nanotechnol.* **2010**, *5*, 574–578.
9. Ishikawa, K. L. Nonlinear Optical Response of Graphene in Time Domain. *Phys. Rev. B* **2010**, *82*, 201402(R).
10. Avetissian, H. K.; Avetissian, A. K.; Mkrtchian, G. F.; Sedrakian, Kh. V. Creation of Particle-Hole Superposition States in Graphene at Multiphoton Resonant Excitation by Laser Radiation. *Phys. Rev. B* **2012**, *85*, 115443.
11. Liu, M.; Yin, X.; Ulin-Avila, E.; Geng, B.; Zentgraf, T.; Ju, L.; Wang, F.; Zhang, X. A Graphene-Based Broadband Optical Modulator. *Nature* **2011**, *474*, 64–67.
12. Mueller, T.; Xia, F.; Avouris, P. Graphene Photodetectors for High-Speed Optical Communications. *Nat. Photonics* **2010**, *4*, 297–301.
13. Sun, Z.; Hasan, T.; Torrisi, F.; Popa, D.; Privitera, G.; Wang, F.; Bonaccorso, F.; Basko, D. M.; Ferrari, A. C. Graphene Mode-Locked Ultrafast Laser. *ACS Nano* **2010**, *4*, 803–810.
14. Gu, T.; Petrone, N.; McMillan, J. F.; van der Zande, A.; Yu, M.; Lo, G. Q.; Kwong, D. L.; Hone, J.; Wong, C. W. Regenerative Oscillation and Four-Wave Mixing in Graphene Optoelectronics. *Nat. Photonics* **2012**, *6*, 554–559.
15. Nair, R. R.; Blake, P.; Grigorenko, A. N.; Novoselov, K. S.; Booth, T. J.; Stauber, T.; Peres, N. M. R.; Geim, A. K. Fine Structure Constant Defines Visual Transparency of Graphene. *Science* **2008**, *320*, 1308.
16. Ferrari, A.; Meyer, J.; V. Scardaci, V.; Casiraghi, C.; Lazzeri, M.; Mauri, F.; Piscanec, S.; Jiang, D.; Novoselov, K.; Roth, S.; *et al.* Raman Spectrum of Graphene and Graphene Layers. *Phys. Rev. Lett.* **2006**, *97*, 187401.
17. Ferrari, A. Raman Spectroscopy of Graphene and Graphite: Disorder, Electron—Phonon Coupling, Doping and Non-adiabatic Effects. *Solid State Commun.* **2007**, *143*, 47–57.
18. Malard, L.; Pimenta, M.; Dresselhaus, G.; Dresselhaus, M. Raman Spectroscopy in Graphene. *Phys. Rep.* **2009**, *473*, 51–87.
19. Dresselhaus, M.; Jorio, A.; Hofmann, M.; Dresselhaus, G.; Saito, R. Perspectives on Carbon Nanotubes and Graphene Raman Spectroscopy. *Nano Lett.* **2010**, *10*, 751–758.
20. Denk, W.; Strickler, J. H.; Webb, W. W. Two-Photon Laser Scanning Fluorescence Microscopy. *Science* **1990**, *248*, 73–76.
21. Jung, J. C.; Schnitze, M. J. Multiphoton Endoscopy. *Opt. Lett.* **2003**, *28*, 902–904.
22. Helmchen, F.; Denk, W. Deep Tissue Two-Photon Microscopy. *Nat. Methods* **2005**, *2*, 932–940.
23. Zipfel, W.; Williams, R.; Webb, W. W. Nonlinear Magic: Multiphoton Microscopy in the Biosciences. *Nat. Biotechnol.* **2003**, *21*, 1369–1377.
24. Liu, W.-T.; Wu, S. W.; Schuck, P. J.; Salmeron, M.; Shen, Y. R.; Wang, F. Nonlinear Broadband Photoluminescence of Graphene Induced by Femtosecond Laser Irradiation. *Phys. Rev. B* **2010**, *82*, 081408(R).
25. Lui, C. H.; Mak, K. F.; Shan, J.; Heinz, T. F. Ultrafast Photoluminescence from Graphene. *Phys. Rev. Lett.* **2010**, *105*, 127404.
26. Dean, J. J.; van Driel, H. M. Second Harmonic Generation from Graphene and Graphitic Films. *Appl. Phys. Lett.* **2009**, *95*, 261910.
27. Hong, S.-Y.; Dadap, J. I.; Petrone, N.; Yeh, P.-C.; Hone, J.; Osgood, R. M., Jr. Optical Third-Harmonic Generation in Graphene. *Phys. Rev. X* **2013**, *3*, 021014.
28. Kumar, N.; Kumar, J.; Gerstenkorn, C.; Wang, R.; Chiu, H.-Y.; Smirl, A. L.; Zhao, H. Third Harmonic Generation in Graphene and Few-Layer Graphite Films. *Phys. Rev. B* **2013**, *87*, 121406(R).
29. Blake, P.; Hill, E.; Castro Neto, A.; Novoselov, K.; Jiang, D.; Yang, R.; Booth, T.; Geim, A. Making Graphene Visible. *Appl. Phys. Lett.* **2007**, *91*, 063124-1–3.
30. Hendry, E.; Hale, P. J.; Moger, J.; Savchenko, A. K.; Mikhailov, S. A. Coherent Nonlinear Optical Response of Graphene. *Phys. Rev. Lett.* **2010**, *105*, 097401.
31. Rajkanan, K.; Singh, R.; Shewchun, J. Absorption Coefficient of Silicon for Solar Cell Calculations. *Solid-State Electron.* **1979**, *22*, 793–795.
32. Dinu, M.; Quochi, F.; Garcia, H. Third-Order Nonlinearities in Silicon at Telecom Wavelengths. *Appl. Phys. Lett.* **2003**, *82*, 2954.
33. Jeschke, H. O.; Garcia, M. E.; Bennemann, K. H. Theory for the Ultrafast Ablation of Graphite Films. *Phys. Rev. Lett.* **2001**, *87*, 015003.
34. Li, X.; Cai, W.; An, J.; Kim, S.; Nah, S.; Yang, D. P.; Velamakanni, A.; Jung, I.; Tutuc, E.; Banerjee, S.; *et al.* Large-Area Synthesis of High-Quality and Uniform Graphene Film on Copper Foils. *Science* **2009**, *324*, 1312–1314.
35. Novoselov, K. S.; Geim, A. K.; Morozov, S. V.; Jiang, D.; Zhang, Y.; Dubonos, S. V.; Grigorieva, I. V; Firsov, A. A. Electric Field Effect in Atomically Thins Carbon Films. *Science* **2004**, *306*, 666–669.
36. Kieu, K.; Jones, J.; Peyghambarian, N. Generation of Few-Cycle Pulses from an Amplified Carbon Nanotube Mode-Locked Fiber Laser System. *IEEE Photonics Technol. Lett.* **2010**, *22*, 1521–1523.
37. Kieu, K.; Mansuripur, M. Femtosecond Laser Pulse Generation with a Fiber Taper Embedded in Carbon Nanotube/Polymer Composite. *Opt. Lett.* **2007**, *32*, 2242–2244.